This article has been accepted for publication in a future issue of this journal, but has not been fully edited. Content may change prior to final publication. Citation information: DOI 10.1109/JIOT.2020.3023105, IEEE Internet of Things Journal

Automatic Detection of Congestive Heart Failure Based on a Hybrid Deep Learning Algorithm in the Internet of Medical Things

Wenlong Ning, Shuhua Li, Dongmei Wei, Long Zhe Guo, Hong Chen

***Abstract*—Congestive heart failure (CHF) is a chronic heart condition with heart function decline caused by various heart diseases that requires long-term treatment and affects personal life safety. At present, CHF diagnosis is being conducted by experts, which is a nonspecific mode that is time consuming and depends on experience. Therefore, it is of great clinical value to conduct CHF recognition through automatic detection. This paper proposed an automatic CHF detection model based on a hybrid deep learning algorithm that is composed of a convolutional neural network (CNN) and a recursive neural network (RNN). We also classified normal sinus heart rate signals and CHF signals based on electrocardiography (ECG) and time-frequency spectra during the RR interval. The accuracy of this algorithm was 99.93%, the sensitivity was 99.85% and the specificity was 100% when 5 min ECG signals were analyzed. It showed a certain improvement over previous studies. We also investigated the detection of CHF patients from healthy subjects by ultrashort-term ECG, and good performance was obtained. The hybrid deep learning algorithm can make objective, accurate classifications of CHF signals and serve as an effective auxiliary tool for the clinical detection of CHF patients.**

***Index Terms*—Congestive Heart Failure; Hybrid Deep Learning; Automatic Detection; Internet of Medical Things**

I. INTRODUCTION

Congestive heart failure (CHF) is characterized by a decrease in heart stroke volume caused by a decline in ventricle blood pumping function. As a result, blood perfusion is insufficient for body tissues and organs, and normal functions are influenced. It can even lead to death. Worldwide, over 26 million people contract CHF every year. Every 5 years, nearly half of the patients will die [1-3]. The symptoms of these patients depend on the CHF severity. Obvious symptoms are present only when the disease becomes very severe, namely, grade 3 or grade 4 CHF. Cardiologists can determine whether a patient has CHF based on some typical features, but the accuracy depends on their ability and experience. In addition, it requires considerable time and effort. In addition, some symptoms of CHF may be similar to geriatric diseases, which can lead to delays in treatment [4]. Therefore, it is of great clinical value to study CHF automatic detection.

Electrocardiography (ECG) is an important technical method for detecting heart-related diseases. Under normal physiological statuses, heart rhythm is controlled through coordination of sympathetic nerves and parasympathetic nerves, two branches of the autonomic nervous system, and diseases will disrupt the coordination and balance. Such rhythmical phenomena can be quantified through the analysis of heart rate variability (HRV). In other words, HRV can express fluctuations in heart rates caused by regulation of the autonomic nervous system, based on which physiological and pathological heart states can be analyzed [5]. In general, HRV analysis is called a time sequence of an RR interval, namely, a time sequence composed of continuous R-wave intervals extracted from ECG signals, and it is widely applied in detecting disease [6,7] and prognosis [8,9]. HRV analysis is a noninvasive and useful tool that can reflect an ANS state [10], so it is often applied in studying CHF [11,12]. Analysis methods of HRV sequences mainly include linear analysis methods including time-domain analysis and frequency-domain analysis, nonlinear analysis methods including detrended fluctuation analysis and recurrent quantitative analysis, entropy analysis methods such as approximate entropy, sample entropy and fuzzy entropy [13], and heart rate asymmetry analysis [14]. Time-domain indexes have shown that HRV is obviously lower [15], frequency-domain indexes have shown that HRV of CHF patients differ obviously from healthy patients [16], and similar results have been obtained through nonlinear analysis methods [17]. These studies provide a theoretical foundation for the detection of CHF patients with HRV.

The development of machine learning technologies has provided a powerful tool for classification. Asyali et al. [18] extracted 9 time-domain and frequency-domain indexes from the RR interval sequence, wherein linear discriminant analysis and a Bayes classifier were used to study the long-term HRV sequence to classify CHF patients and healthy subjects. Isler et

Wenlong Ning and Long Zhe Guo are with the Department of Cardiology, The First Hospital of Qiqihar, Qiqihar, China; and the Department of Cardiology, Affiliated Qiqihar Hospital, Southern Medical University, Qiqihar, China (Email: wenlong_ning@muc.edu.cn, guolongzhe0502@163.com)

Shuhua Li, Dongmei Wei and Hong Chen are with the Department of Traditional Chinese Medicine, The First Hospital of Qiqihar, Qiqihar, China; and the Department of Traditional Chinese Medicine, Affiliated Qiqihar Hospital, Southern Medical University, Qiqihar, China (Email: lishuhua0502@163.com, weidongmei_1979@163.com, and chenhong_1964@163.com).

Corresponding author: Long Zhe Guo and Hong Chen (Email: guolongzhe0502@163.com and chenhong_1964@163.com). Long Zhe Guo and Hong Chen contributed equally to this article as co-corresponding authors.

This article has been accepted for publication in a future issue of this journal, but has not been fully edited. Content may change prior to final publication. Citation information: DOI 10.1109/JIOT.2020.3023105, IEEE Internet of Things Journal

al. [19] extracted time-domain and frequency-domain indexes from a short-time RR interval and studied CHF classification through wavelet entropy and the nearest neighbor algorithm. Altan et al. [20] studied the application of the Hilbert-Huang transformation of HRV signals in CHF analysis using artificial neural networks. Narin et al. [21] studied CHF using the support vector machine (SVM) algorithm, wherein input features were traditional time-domain, frequency-domain and nonlinear analysis results. Acharya et al. [22] used the empirical mode decomposition of HRV signals to complete research based on probabilistic neural networks and SVMs. Isler et al. [23] computed features such as the time-domain and frequency domain of HRV, Poincare map, symbol dynamics, nontrend fluctuation analysis, and sample entropy nonlinearity and detected CHF with a multilevel classifier. Li et al. [24] used a deep learning classifier based on a convolutional neural network (CNN) to study HRV recognition in CHF patients. Meillo et al. [25] confirmed CHF patients with a CART classifier. Chen et al. [26] extracted features from short-term heart rate signals through a sparse autoencoder and detected heart failure based on a deep learning algorithm. The mentioned detection methods are deficient in accuracy, and the models are highly complicated and consume a long time for computation.

In this paper, features were extracted from ECG, mainly the RR interval sequence, time spectra of ECG signals were computed, and CNN was used to automatically recognize spectra crossed with time domains as well as relevant features. A CNN is a feedforward neural network that performs well in processing larger images and has been widely applied to image classification and positioning. Compared with other neural network structures, the CNN stands out because of fewer parameters. A recursive neural network (RNN) is an artificial neural network that has a tree-shaped hierarchical structure, wherein its network nodes conduct recursion of input information according to a connection sequence. It is deemed a promoted type of recurrent neural network [27]. When each father node of an RNN is connected to only one subnode, its structure is equivalent to a fully connected recurrent neural network. The time spectrum has a digital matrix similar to an image, while features correlated with specific physiological states are formed in specific subareas. Therefore, in this work, these features were recognized with a hybrid deep learning algorithm that combined CNN and RNN. CHF classification was conducted by combining other features.

The overall organization of this work is as follows. The second section introduces the collected data from the Internet of Medical Things. The third section discusses the material and methods adopted by this paper. The fourth section presents some computed results. The fifth section presents some discussion and explains the computed results. The last section concludes and presents future work.

II. Data Source from the Internet of Medical Things

The data source in this work is collected from the Internet of Medical Things, as shown in Figure 1. As seen in this figure, many sensors are located on the heart to detect ECG signals. We also located other sensors for collecting electroencephalogram signals. However, in this work, we only study the automatic detection of CHF, so we complete the work based on the ECG signal.

The experimental data in this work are divided into two parts. One part is from 15 CHF patients, and another part is from 18 healthy subjects with normal sinus rhythm (NSR). ECG signals of 15 patients with severe CHF, including 11 males aged 22-71 and 4 females aged 54-63 are adopted. Signals were collected after approximately 20 hours. Each record includes two channels of ECG, with a sampling rate of 250 Hz. Additional subjects involved in the data collection were healthy people with normal sinus rhythm, including 5 males aged 26-45 and 13 females aged 20-50, with a sampling rate of 128 Hz.

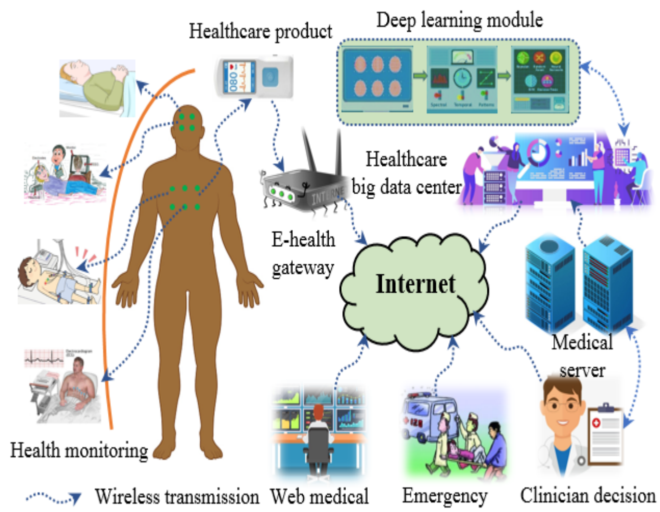

Fig. 1 Data collection from the Internet of Medical Things

According to clinical requirements, we conducted CHF detection based on short-term continuous heart rate data in this work. As shown in the research, time sequences shorter than 30 min are short-time sequences. Five minutes is an acknowledged length for short HRV time-series analysis, and 1 min is a common choice for ultrashort HRV analysis. Therefore, we conducted a nonrepeated division of the long-term sequence. Every 5 min was selected as a section. The last section was removed if it was not longer than 5 min. There were 4,603 segments of data in the healthy group, and the CHF group had 3,575 segments of data for 5 min HRV analysis. There were 23,017 and 17,878 segments of healthy subjects and CHF subject data, respectively, for 1 min HRV analysis. Although the data have some imbalance with using all data, it is acceptable to use as much data as possible.

III. Materials and Methods

A. *Preprocessing and Extracting R Waves*

The R-wave peak is a point in ECG signals that can be marked easily. Sets composed of distances between R waves become time sequences that are most commonly used in studying an autonomic neural system, namely, RR interval sequences. They are constructed as shown in Figure 2. Before extracting R waves, the signals were preprocessed. Noise signals in ECG signals were removed through preprocessing of a finite impulse response (FIR) low-pass filter with a cut-off frequency of 22 Hz and a FIR high-pass filter with a frequency of 1.2 Hz. After that, frequency interference in the ECG signals was removed by a 60 Hz notching filter. Finally, baseline drift was removed. The most advanced QRS wave detector was used for detecting the ECG R-wave peak [28], which improved the results by over 4% for F_1 compared to the best single-lead ECG QRS detector. The detector was composed of a peak energy detector based on windows and had very strong robustness for noise. To avoid any impact on the performance of the time-frequency-domain index, the abnormal intervals were removed for RR intervals before analysis. Abnormal values caused by incorrect or missed detection of the R-wave peak were removed by a sliding window average filter with a length of 41. Center points exceeding 20% of the window on average were removed. Figure 3 shows the original signals and preprocessed information as well as marked positions of the R-wave peak.

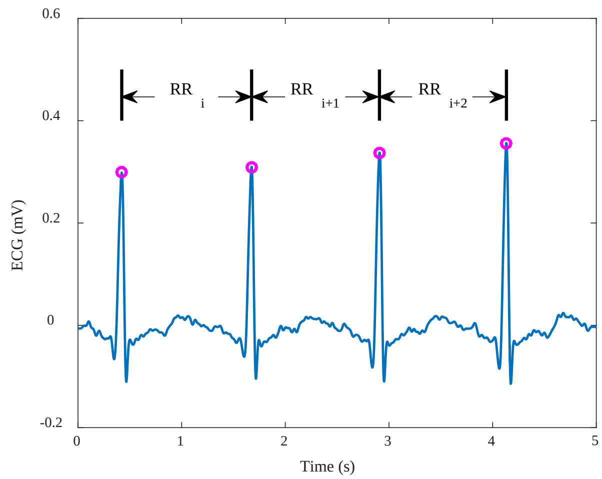

Fig. 2 Construction of RR interval sequences

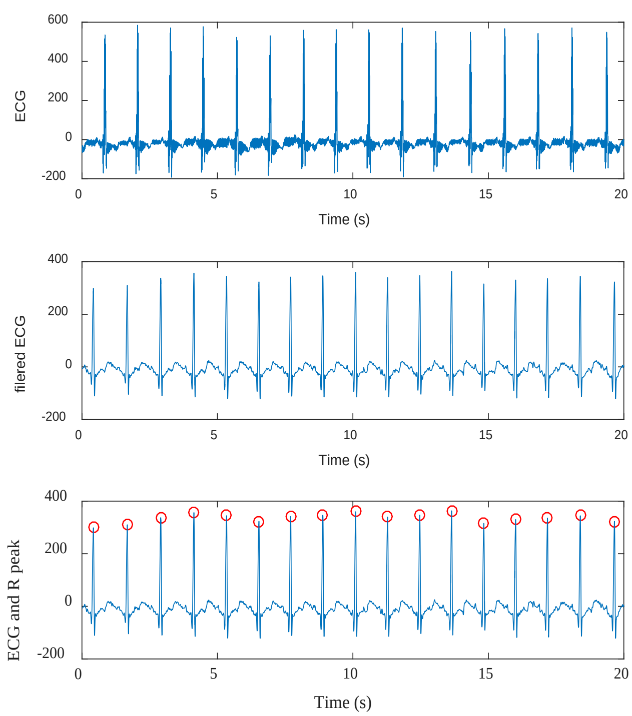

Fig. 3 Original ECG, filtered ECG and RR wave peak

B. Construction and Feature Extraction of RR Interval Time Sequences

1) Time-domain index

The time-domain method is the earliest method used for studying HRV. With simple computation, this method can provide useful information. The index's standard deviation of normal-normal intervals (SDNN) and the square root of the mean squared differences (RMSSD) are commonly used. The computing formula is as follows:

SDNN intervals indicate the standard deviation of the time sequence:

$$SDNN = \sqrt{\frac{1}{N}\sum_{i=1}^{N}(NN_i - NN_{mean})^2}, i = 1,2,..,N \quad (1)$$

In Equation (1), N is the length of the RR interval sequence. NN_i is the RR interval of the i-th normal sinus heart rate. NN_{mean} is the mean value of the normal sinus heart rates in the RR interval.

RMSSD is the square root of the mean squared differences of neighboring RR intervals.

$$RMSSD = \sqrt{\frac{\sum_{i=1}^{N-1}(RR_{i+1} - RR_i)^2}{N-1}} \quad (2)$$

2) Frequency-domain index

Frequency-domain analysis methods aim to analyze the power frequency spectrum density in a frequency domain, which is transformed from a time sequence based on discrete Fourier transformation (DFT). The RR interval spectrum is mainly divided into high-frequency components (0.15-0.40 Hz), which reflect the activity of parasympathetic nerves, and low-frequency components (0.04-0.15 Hz), which are simultaneously regulated by the sympathetic and parasympathetic nervous. Frequency-domain analysis has been widely used in the analysis of the regulatory functions of autonomic nerves. Indexes including low frequency (LF), high frequency (HF) and HF/LF are commonly used. HF indicates components with a spectral scope of 0.04-0.15 Hz in an HRV signal power spectrum, LF (low frequency) represents components with a spectral scope of 0.15-0.40 Hz in an HRV signal power spectrum, and HF/LF denotes a ratio of HF to LF components. According to the frequency-domain analysis of 5 min ECG signals, HF components generally reflect the activity of parasympathetic nerves, while LF components are simultaneously regulated by sympathetic and parasympathetic nervous systems.

3) Nonlinear method

The physiological system is a nonlinear system. The cardiovascular system is regulated by the endocrine system and body fluids of the autonomic nervous system. It is a steady-state balance system with highly complex nonlinear characteristics and dynamic behavior. Any functional degradation in the cardiovascular system will reduce the balance in the entire system, resulting in the loss of its corresponding nonlinear properties and changes in its dynamic behavior. Its dynamic changes cannot be measured with time and frequency only.

Nonlinear features of time sequences are computed with nonlinear methods. Features of time sequences are depicted from perspectives such as fractals and complexity of time sequences. Outstanding achievements have been obtained. There are many methods for analyzing nonlinear features of time sequences. In this work, a Poincare map that describes a chaotic feature of the time sequence was selected as a nonlinear index. In the Poincare map, geometric features of scattering points in a map are quantified, while features are described from the perspective of the map. The Poincare map of RR interval sequences involves scattering points that are distributed relative to a symmetric line that has a gradient of 45° and passes the origin point. For an RR interval sequence $\{RR_1, RR_2, \ldots, RR_i, RR_{i+1}, \ldots, RR_{N-1}, RR_N, 1 \leq i \leq N\}$ with a length of N, the i-th scattering point in the figure can be denoted as $[RR_i, RR_{i+1}]$. As shown in Figure 4, HRV was measured through ellipse fitting. The long axis SD1 of the ellipse denotes the long-time variance in the RR interval, namely, the length of the line along the 45° linear direction. The short axis SD2 denotes the short-time variance in the HRV, namely, the length of the line perpendicular to the 45° straight line. Their ratio is often used to measure the HRV, namely, $SD1/SD2$. It is computed as follows:

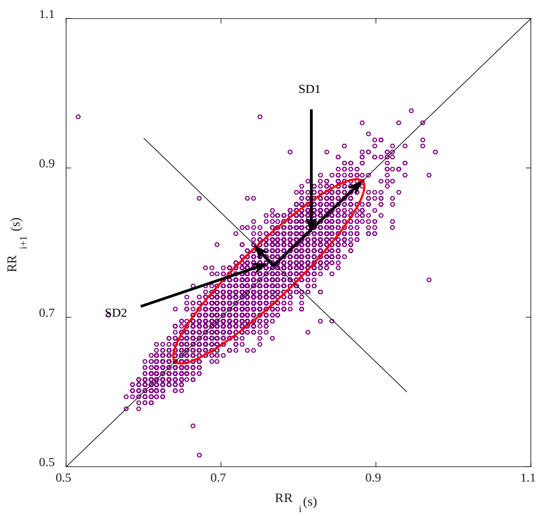

Fig. 4 Schematic diagram of the Poincare map. The data were chosen from a healthy subject that was selected randomly. The point was set to the *i*th RR interval as the x-axis and the *i*+1th RR interval as the y-axis.

$$SD1 = \sqrt{VAR\frac{RR_i - RR_{i+1}}{\sqrt{2}}} \quad (3)$$

$$SD2 = \sqrt{VAR\frac{RR_i + RR_{i+1}}{\sqrt{2}}} \quad (4)$$

$$SD1/SD2 = \frac{SD1}{SD2} \quad (5)$$

As proposed by Karmakar, the slope index (SI) can measure the asymmetry between the HRV scattering point in the Poincare map and a symmetric included angle [14]. SI is an algorithm used to measure the geometric structure of the scattering point distribution in the Poincare map.

$$SI = \frac{\sum_{i=1}^{l}|R\theta_i|}{\sum_{i=1}^{n}|R\theta_i|} \times 100 \quad (6)$$

In this equation, l is the number of points above the symmetric line L_i (namely, $\Delta RR > 0$). n is the number of points that are not located on the symmetric line L_i (namely, the part other than $\Delta RR = 0$), $R\theta_i = \theta_{Li} - \theta_i$. θ_{Li} is the angle of L_i and is equal to 45°. θ_i is the angle of the i-th point, $\theta_i = atan(RR_{i+1}/RR_i)$, as shown in Figure 5.

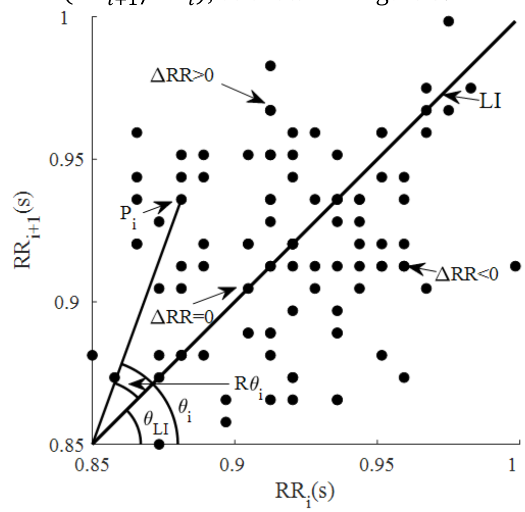

Fig. 5 Schematic diagram of SI in the Poincare map. The data were chosen from a healthy subject that was selected randomly. The point was set to the *i*th RR interval as the x-axis and the *i*+1th RR interval as the y-axis.

4) *Time-frequency spectrum of ECG signals*

Images can be processed with CNN, so ECG signals were transformed into images in this work. For this purpose, time-frequency spectra were used. With time-frequency spectra, changes in signal powers in an image can be captured through the Fourier transform of each part of the signals. The number of divided areas can be deemed an adjustable hyperparameter that depends on signal details and relevant changes of signals between categories. The short-time Fourier transform was used to obtain the time-frequency spectra. The longer the window, the worse the time resolution was and the better the frequency resolution. Here, the length of the sliding window was set to 32. Time-frequency spectra of healthy and CHF subjects are shown in Figure 6.

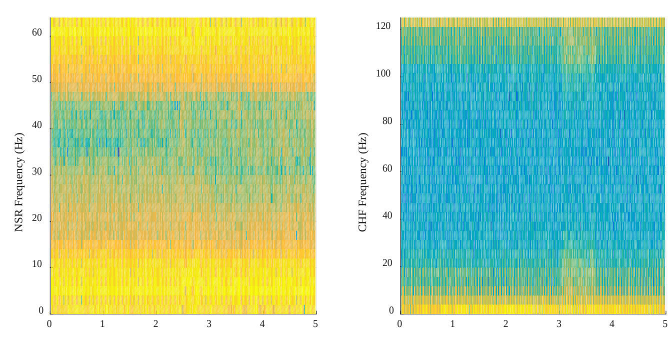

Fig. 6 Frequency spectra of ECG signals for healthy and CHF subjects in 5 min; the left is healthy subjects and the right is CHF subjects. Hotter colors indicate a higher spectrum.

This article has been accepted for publication in a future issue of this journal, but has not been fully edited. Content may change prior to final publication. Citation information: DOI 10.1109/JIOT.2020.3023105, IEEE Internet of Things Journal

5) Time-frequency spectra of the RR interval

Similar to ECG signals, in the time-domain spectra of RR intervals used in this paper, the RR interval time sequence was mapped from a one-dimensional structure to two-dimensional planar space, and this figure was taken as the input of CNN. The time-frequency spectra of the RR interval for healthy and CHF subjects are shown in Figure 7. The left figure shows the time-frequency spectrum of healthy subjects. The right figure shows the time-frequency spectrum of CHF subjects.

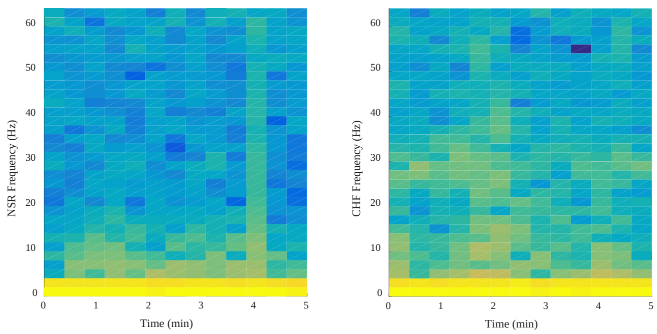

Fig. 7 Time-frequency spectra of RR intervals for healthy and CHF subjects in 5 min; the left is healthy subjects, and the right is CHF subjects. Hotter colors indicate a higher spectrum.

C. Statistical Analysis

We applied the algorithms and plotted the figures in MATLAB (Ver. R2016a, Mathworks Inc, MA, USA). For a single index, all results were verified by the Shapiro-Wilk test, and they did not conform to a normal distribution. Hence, the nonparameter Wilcoxon signed-rank test was used to compare the differences of CHF patients in time-domain, frequency-domain and nonlinear indexes with NSR groups. $p < 0.05$ a significant difference between CHF and NSR; $p < 0.01$ is a highly significant difference. Differentiation effects of indexes were further measured with AUC (area under the receiver operating characteristic curve (ROC) curve). A closer approach of the AUC to 1 indicates a better differentiation effect. These results were used for the proposed hybrid deep learning model.

D. Hybrid Deep Learning Algorithm

CNN is an improvement to an error backpropagation network [29]. The CNN proposed by Yann Lecun et al. applies layers with convolutional filters and is applied to local features [30]. The CNN model, which was originally invented for computer vision, was later proven to be valid for natural language processing and obtained very good effects in semantic parsing [31], search, query and retrieval [32], sentence modeling [33] and other traditional tasks for natural language processing [34]. CNNs are effective because of the ability to learn abundant middle-level image expressions rather than low-layer features of artificial design used in other image classification methods. With a tree-like neural network structure, RNN realizes the recursion of a complicated deep network. Essentially, CNN represents a valid expansion of recurrent neural networks. They have different computational diagrams. A hybrid deep learning algorithm combining CNN and RNN, which integrates the advantages of the two models, is proposed for the automatic detection of CHF patients. The network structure used in this paper is shown in Figure 8, and it is drawn based on previous work [35]. The number of training parameters is 84,630,256, the learning rate is 10^{-4}, and the number of iterations is set to 30,000. All experiments were performed on a PC with a Windows 10 operating system, a 2.6 GHz Intel Core i7 CPU, 16 GB RAM, and an NVIDIA GeForce GTX 2080Ti GPU.

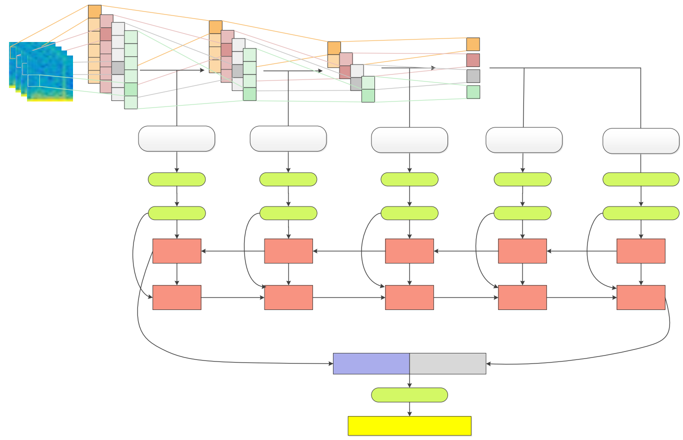

Fig. 8 Architecture of the proposed hybrid deep learning algorithm

IV. Results

An HRV result with a continuous length of 5 min was randomly extracted from the ECG signals with a length over 20 hours, as shown in Figure 9. Obviously, there was no significant difference between RMSSD and SD1 ($p > 0.05$), while the other 7 indexes showed significant differences ($p < 0.05$). According to this result, 7 different indexes can effectively facilitate CHF detection. The results show that the Poincare maps of CHF patients were obviously different from the baseball-shaped structure of healthy subjects [36, 37]. The results also support our conclusion. As shown in Figure 9(i)), the SI of CHF patients increased, indicating a loss of balance in their heart rate regulation ability. The ROC curve shown in Figure 10 indicates $AUC > 0.65$ for 7 indexes. Hence, we can use these 7 indexes as features of CHF detection.

A continuous ECG section with a length of 1 min was selected randomly from the data, and the RR interval was extracted for analysis, as shown in Figure 11 and Figure 12. As an exception, the SI results of the 1 min HRV sequence did not show any significant difference, indicating the poor ability of SI in supershort time sequence analysis; the difference in HF/LF changed from $p < 0.001$ to $p < 0.05$, with a decrease. The analyzed results of other indexes were the same as the results for 5 min. Therefore, during ECG classification for healthy and CHF subjects using the 1 min ECG data, we input 6 indexes (SDNN, RMSSD, HF, HF/LF, SD2 and SD1/SD2) in combination with time-frequency spectra of ECG signals and RR intervals.

This article has been accepted for publication in a future issue of this journal, but has not been fully edited. Content may change prior to final publication. Citation information: DOI 10.1109/JIOT.2020.3023105, IEEE Internet of Things Journal

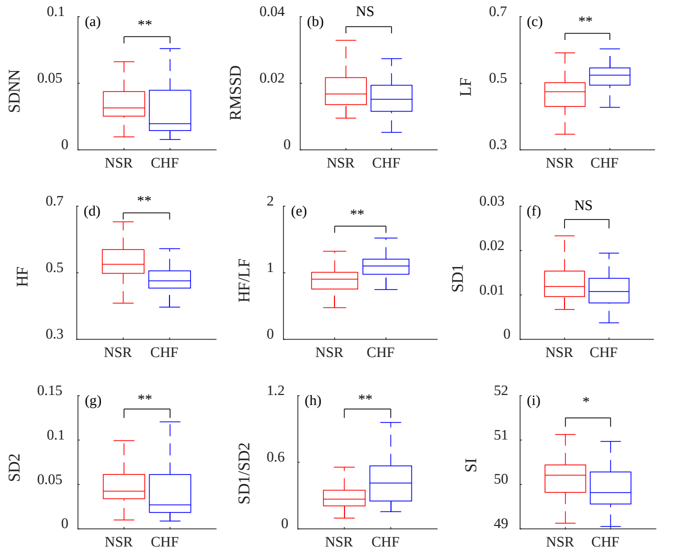

Fig. 9 HRV results of 5 min NSR and CHF with different indexes. (a) SDNN, (b) RMSSD, (c) LF, (d) HF, (e) HF/LF, (f) SD1, (g) SD2, (h) SD1/SD2, (i) SI. $*$ is $p < 0.05$, $**$ is $p < 0.001$, NS: no significant difference.

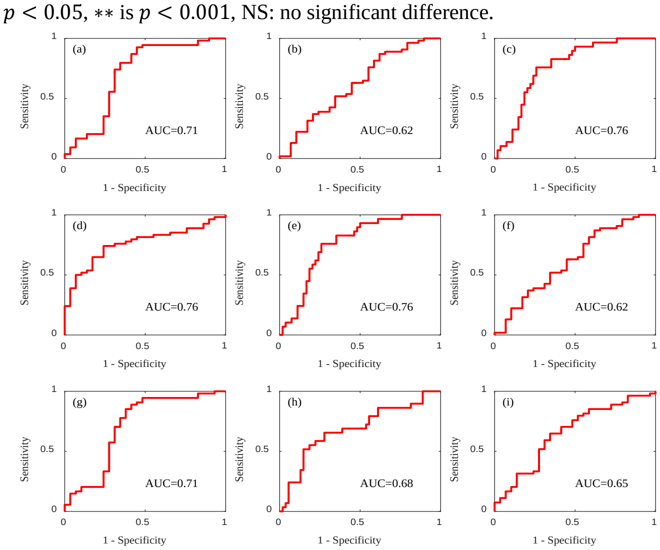

Fig. 10 ROC curves of HRV of 5 min NSR and CHF with different indexes. (a) SDNN, (b) RMSSD, (c) LF, (d) HF, (e) HF/LF, (f) SD1, (g) SD2, (h) SD1/SD2, (i) SI.

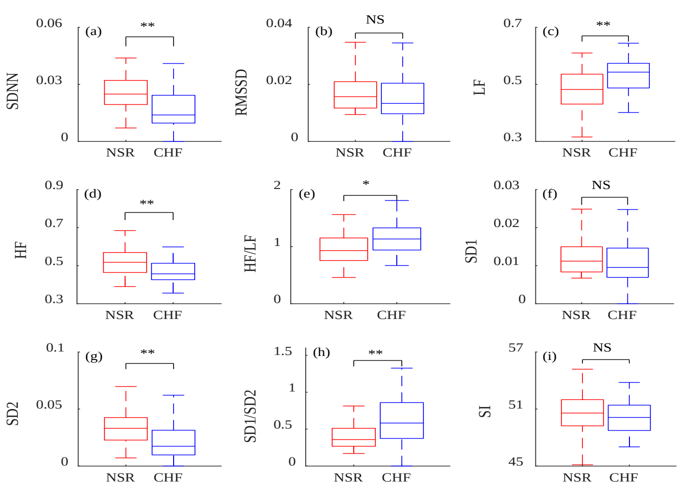

Fig. 11 HRV results of 1 min NSR and CHF with different indexes. (a) SDNN, (b) RMSSD, (c) LF, (d) HF, (e) HF/LF, (f) SD1, (g) SD2, (h) SD1/SD2, (i) SI. $*$ is $p < 0.05$, $**$ is $p < 0.001$, NS: no significant difference.

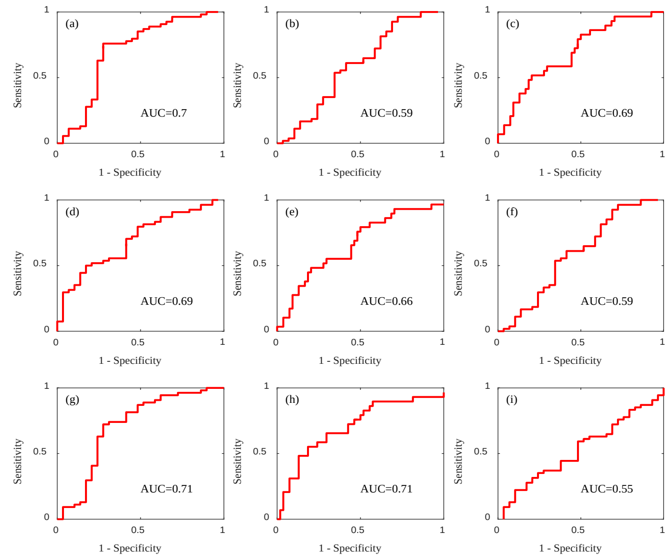

Fig. 12 ROC curves of 1 min NSR and CHF with different indexes. (a) SDNN, (b) RMSSD, (c) LF, (d) HF, (e) HF/LF, (f) SD1, (g) SD2, (h) SD1/SD2, (i) SI.

The results of these methods were combined with ECG time-frequency spectra. Classified results with the proposed hybrid deep learning algorithm were computed. Accuracy, sensitivity and specificity are chosen as the evaluation indexes because they are convenient for comparison with previous studies. In addition, these three indexes are commonly used clinical quantification indexes and algorithm performance standards. For differentiation of normal sinus rhythm and CHF data, the accuracy was 99.93%, the sensitivity was 99.85%, and the specificity was 100%. Through comparison of the results with other traditional methods, matched accuracies were obtained, as shown in Table 1.

TABLE 1
COMPARISON RESULTS BETWEEN THE PROPOSED METHOD AND OTHER TRADITIONAL METHODS

Methods	Accuracy (%)	Sensitivity (%)	Specificity (%)
This paper (5 min)	99.93	99.85	100%
This paper (1 min)	98.50	97.96	99.08
Acharya, et al. [22]	94.40-98.97^{b}	94.68-98.87^{b}	95.75-99.01^{b}
Sudarshan et al.[38]	97.94-99.87^{b}	97.04-99.78^{b}	97.69-99.94^{b}
Masetc et al.[39]	100.00	NP	NP
Kamath et al.[40]	79.20-98.20^{b}	71.50-98.40^{b}	87.80-98.00^{b}

b: the range of results obtained from several different datasets; NP: not reported.

V. DISCUSSIONS

In this study, time-domain indexes (SDNN and RMSSD), frequency-domain indexes (LF, HF and HF/LF) and nonlinear indexes (Poincare map and SI), as well as the time-frequency spectrum of ECG signals in combination with the hybrid deep learning algorithm, were used for CHF detection. These indexes denote the decline in autonomic nervous functions of CHF patients, which was significantly different from healthy subjects. This result provided a feasible method for CHF detection or even earlier prediction and conformed to most previous studies.

In comparison with many other studies, we used fewer features, including 5 linear indexes, 2 nonlinear indexes and time-frequency spectra of ECG signals, which were rarely reported. The application of this figure is advantageous in that the algorithm complexity is increased for different modes of feature extraction from ECG, particularly HRV signal analysis. Only information contained in RR intervals is analyzed. The time-frequency spectra make use of ECG signals and time-domain and frequency-domain information more frequently than traditional algorithms. In addition, the hybrid deep learning algorithm has unique advantages in processing images and videos. Therefore, through the generation of images and input into this algorithm, algorithm characteristics can be fully utilized to positively promote results. In addition, very high accuracy is achieved without considering the impact of the sensor, which provides a good explanation for the clinical value of our algorithm.

In addition, the methods were used in some reports (such as Table 1) for only a very short time, while results with high accuracy or even 100% accuracy were achieved. As for this point, the study may have weaknesses. However, data collection of 5 min or 1 min clinical demands for disease detection can contain more abundant information than that in a very short time. As we deduced, this proposed algorithm will have a very stable generalization ability, which needs further verification.

There are some limitations to this study. First, ECG data of 5 min and 1 min were used for CHF detection. The results can meet clinical demands, but model verification was not conducted aiming at shorter-time ECG data. In clinical applications, a detection mode for a supershort time is necessary to relieve clinical stress, save time for doctors and bring convenience to more patients. Second, abnormal values were eliminated during extracting the RR interval. In measurement, various types of noise may exist. Moreover, with the generalization of wearable equipment, signal collection may face more complicated and variable environments. Therefore, the generalization ability of this model for abnormal signals such as those containing noise still needs further verification. Third, CHF data from patients with grade 3 and grade 4 CHF were used. Whether the method can be applied to earlier CHF detection was not confirmed and will become a hot topic in the future. Fourth, the number of samples in this study was fewer than 20. We cut the original data into 5 min or 1 min segments to increase the quantity of data and verify the effect of the model. The purpose was to make the number of samples meet the requirements of training and testing of deep learning. The results prove that our proposed model can detect heart failure very well. However, the segmented data may have a certain correlation, so we plan to verify the accuracy of our model on a larger sample set in the future.

In later research, we will use ultrashort ECG signals for CHF detection to relieve the pressure of patient queuing and hospitals and provide referential technologies for increasing the accuracy of patient detection. Additionally, we will add different proportions of noise to normal signals after signal elimination to detect the generalization ability of the model. For example, noise of 5%, 10% and 20% will be added to verify whether the model can still accurately recognize CHF patients. In addition, 50% or more noise will be added to the signals to simulate a real complicated environment. In this case, method failure or accuracy decrease to an unacceptable noise proportion will be confirmed. In this way, reliable suggestions can be provided for use conditions of the model. We will also investigate the impact on data collection by sensor selection, placement and data collection environment in the future.

VI. CONCLUSIONS

In conclusion, we developed an ECG signal-based model that detects CHF with a hybrid deep learning algorithm that can realize the clinical recognition of CHF patients with high accuracy. This algorithm was applied to a data source from the Internet of Medical Things to realize automatic detection. We also found that the autonomic nerve estimation method concerning HRV can facilitate confirmative clinical diagnosis of diseases. In addition, time-frequency spectra of ECG signals can play a useful role in the detection of CHF diseases. All these results support CHF diagnosis with clinical computer assistance. The proposed algorithm was compared with many competitive algorithms. In the future, we will study modeling based on shorter-time ECG recognition of CHF as well as application conditions of the proposed model or propose a more advanced algorithm for detecting CHF.

REFERENCES

[1] A. P. Ambrosy, G. C. Fonarow, J. Butler, et al, "The global health and economic burden of hospitalizations for heart failure: lessons learned from hospitalized heart failure registries," Journal of the American College of Cardiology, vol. 63, no. 12, pp. 1123-1133, Apr. 2014.
[2] D. Mozaffarian, E. J. Benjamin, A. S. Go, et al, "Executive summary: heart disease and stroke statistics—2016 update: a report from the American Heart Association," Circulation, vol. 133, no. 4, pp. 447-454, Jan. 2016.
[3] J. Huang, H. Yin, M. Zhang, et al, "Understanding the economic burden of heart failure in China: impact on disease management and resource utilization," Journal of Medical Economics, vol. 20, no. 5, pp. 549-553, Mar. 2017.
[4] N. D. Gillespie, "The diagnosis and management of chronic heart failure in the older patient," British Medical Bulletin, vol. 75, no. 1, pp. 49-62, Feb. 2006.
[5] A. Plaza-Florido, J. H. Migueles, J. Sacha, et al, "The role of heart rate in the assessment of cardiac autonomic modulation with heart rate variability," Clinical Research in Cardiology, vol. 108, no. 12, pp. 1408-1409, May. 2019.
[6] J. S. Mulcahy, D. E. O. Larsson, S. N. Garfinkel, et al, "Heart rate variability as a biomarker in health and affective disorders: A perspective on neuroimaging studies," Neuroimage, vol. 202, pp. 116072, Nov. 2019.
[7] D. P. Barnaby, S. M. Fernando, C. L. Herry, et al, "Heart rate variability, clinical and laboratory measures to predict future deterioration in patients presenting with sepsis," Shock, vol. 51, no. 4, pp. 416-422, Apr. 2019.
[8] W. Chen, L. Zheng, K. Li, et al, "A novel and effective method for congestive heart failure detection and quantification using dynamic heart rate variability measurement," PloS One, vol. 11, no. 11, pp. e0165304, Nov. 2016.
[9] J. P. Saul, Y. Arai, R. D. Berger, et al, "Assessment of autonomic regulation in chronic congestive heart failure by heart rate spectral

analysis," The American journal of cardiology, vol. 61, no. 15, pp. 1292-1299, Jun. 1988.
[10] F. Shahbazi, B. M. Asl, "Generalized discriminant analysis for congestive heart failure risk assessment based on long-term heart rate variability," Computer Methods and Programs in Biomedicine, vol. 122, no. 2, pp. 191-198, Nov. 2015.
[11] A. Koshy, N. C. Okwose, D. Nunan, et al, "Association between heart rate variability and haemodynamic response to exercise in chronic heart failure," Scandinavian Cardiovascular Journal, vol. 53, no. 2, pp. 77-82, Apr. 2019.
[12] G. Casolo, E. Balli, T. Taddei, et al, "Decreased spontaneous heart rate variability in congestive heart failure," The American journal of cardiology, vol. 64, no. 18, pp. 1162-1167, Nov. 1989.
[13] F. Shaffer, J. P. Ginsberg, "An overview of heart rate variability metrics and norms," Frontiers in Public Health, vol. 5, pp. 258, Sep. 2017.
[14] C. K. Karmakar, A. H. Khandoker, M. Palaniswami, "Phase asymmetry of heart rate variability signal," Physiological Measurement, vol. 36, no. 2, pp. 303-314, Jan. 2015.
[15] B. Takase, A. Kurita, M. Noritake, et al, "Heart rate variability in patients with diabetes mellitus, ischemic heart disease, and congestive heart failure," Journal of Electrocardiology, vol. 25, no. 2, pp. 79-88, Apr. 1992.
[16] S. N. Yu, M. Y. Lee, "Bispectral analysis and genetic algorithm for congestive heart failure recognition based on heart rate variability," Computers in Biology and Medicine, vol. 42, no. 8, pp. 816-825, Aug. 2012.
[17] E. Cirugeda-Roldan, D. Cuesta-Frau, P. Miro-Martinez, et al, "Comparative study of entropy sensitivity to missing biosignal data," Entropy, vol. 16, no. 11, pp. 5901-5918, Nov. 2014.
[18] M. H. Asyali, "Discrimination power of long-term heart rate variability measures," Proceedings of the 25th Annual International Conference of the IEEE Engineering in Medicine and Biology Society (IEEE Cat. No. 03CH37439). IEEE, pp. 200-203, Sep. 2003.
[19] Y. İşler, M. Kuntalp, "Combining classical HRV indices with wavelet entropy measures improves to performance in diagnosing congestive heart failure," Computers in Biology and Medicine, vol. 37, no. 10, pp. 1502-1510, Oct. 2007.
[20] G. Altan, Y. Kutlu, N. Allahverdi, "A new approach to early diagnosis of congestive heart failure disease by using Hilbert–Huang transform," Computer Methods and Programs in Biomedicine, vol. 137, pp. 23-34, Dec. 2016.
[21] A. Narin, Y. Isler, M. Ozer, "Investigating the performance improvement of HRV Indices in CHF using feature selection methods based on backward elimination and statistical significance," Computers in Biology and Medicine, vol. 45, pp. 72-79, Feb. 2014.
[22] U. R. Acharya, H. Fujita, V. K. Sudarshan, et al, "Application of empirical mode decomposition (EMD) for automated identification of congestive heart failure using heart rate signals," Neural Computing and Applications, vol. 28, no. 10, pp. 3073-3094, Sep. 2016.
[23] Y. Isler, A. Narin, M. Ozer, et al, "Multi-stage classification of congestive heart failure based on short-term heart rate variability," Chaos, Solitons & Fractals, vol. 118, pp. 145-151, Jan. 2019.
[24] Y. Li, Y. Zhang, L. Zhao, et al, "Combining convolutional neural network and distance distribution matrix for identification of congestive heart failure," IEEE Access, vol. 6, pp. 39734-39744, Jul. 2018.
[25] P. Melillo, R. Fusco, M. Sansone, et al, "Discrimination power of long-term heart rate variability measures for chronic heart failure detection," Medical & Biological Engineering & Computing, vol. 49, no. 1, pp. 67-74, Jan. 2011.
[26] W. Chen, G. Liu, S. Su, et al, "A CHF detection method based on deep learning with RR intervals," 2017 39th Annual International Conference of the IEEE Engineering in Medicine and Biology Society (EMBC). IEEE, pp. 3369-3372, Jul. 2017.
[27] J. B. Pollack, "Recursive distributed representations," Artificial Intelligence, vol. 46, no. 1-2, pp. 77-105, Nov. 1990.
[28] A. E. W. Johnson, J. Behar, F. Andreotti, et al, "Multimodal heart beat detection using signal quality indices," Physiological Measurement, vol. 36, no. 8, pp. 1665-1677, Jul. 2015.
[29] R. Yamashita, M. Nishio, R. K. G. Do, et al, "Convolutional neural networks: an overview and application in radiology," Insights into imaging, vol. 9, no. 4, pp. 611-629, Jun. 2018.
[30] Y. LeCun, Y. Bengio, "Convolutional networks for images, speech, and time series," The Handbook of Brain Theory and Neural Networks, vol. 3361, no. 10, 1995.
[31] W. Yih, X. He, C. Meek, "Semantic parsing for single-relation question answering," Proceedings of the 52nd Annual Meeting of the Association for Computational Linguistics, vol. 2, pp. 643-648, Jun. 2014.
[32] Y. Shen, X. He, J. Gao, et al, "Learning semantic representations using convolutional neural networks for web search," Proceedings of the 23rd international conference on world wide web. pp. 373-374, Apr. 2014.
[33] N. Kalchbrenner, E. Grefenstette, P. Blunsom, "A convolutional neural network for modelling sentences," arXiv preprint arXiv, 1404.2188, Apr. 2014.
[34] R. Collobert, J. Weston, L. Bottou, et al, "Natural language processing (almost) from scratch," Journal of Machine Learning Research, vol. 12, pp. 2493− 2537, Nov. 2011.
[35] X. Zhu, L. Li, W. Zhang, et al, "Dependency exploitation: A unified CNN-RNN approach for visual emotion recognition," Proceedings of the 26th International Joint Conference on Artificial Intelligence, pp. 3595-3601, Aug. 2017.
[36] C. Kamath, "A new approach to detect congestive heart failure using sequential spectrum of electrocardiogram signals," Medical Engineering & Physics, vol. 34, no. 10, pp. 1503-1509, Dec. 2012.
[37] M. Brennan, M. Palaniswami, P. Kamen, "Do existing measures of Poincare plot geometry reflect nonlinear features of heart rate variability," IEEE Transactions on Biomedical Engineering, vol. 48, no. 11, pp. 1342-1347, Nov. 2001.
[38] V. K. Sudarshan, U. R. Acharya, S. L. Oh, et al, "Automated diagnosis of congestive heart failure using dual tree complex wavelet transform and statistical features extracted from 2 s of ECG signals," Computers in Biology and Medicine, vol. 83, pp. 48-58, Apr. 2017.
[39] Z. Masetic, A. Subasi, "Congestive heart failure detection using random forest classifier," Computer Methods and Programs in Biomedicine, vol. 130, pp. 54-64, Jul. 2016.
[40] C. Kamath, "A new approach to detect congestive heart failure using detrended fluctuation analysis of electrocardiogram signals," Journal of Engineering Science and Technology, vol. 10, no. 2, pp. 145-159, Oct. 2015.

Wenlong Ning, Master of medicine, Chief physician. He graduated from Qiqihar Medical College in 1988, bachelor's degree in Harbin Medical University in 1995, and master's degree in 2008. He is the master's supervisor, "national May 1" labor medalist, "Heilongjiang May 1st labor medal", "Heilongjiang famous doctor" and other honorary titles. His published articles are more than 30, including SCI two articles. He edited and published “the modern emergency diagnosis and treatment guide” and “practical arrhythmia diagnosis and treatment guide”, etc. He won thrice second prize of Heilongjiang province science and technology new technology, 4 time of third prize of Heilongjiang province science and technology new technology, twice third prizes of Qiqihar city science and technology progress scientific research achievements, and thrice excellent prizes of Qiqihaer city science and technology achievements.

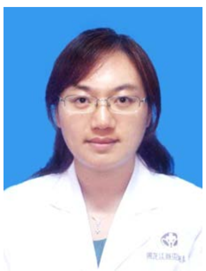

Shuhua Li, Post doctor, PhD of medicine, Deputy chief physician. She obtained a bachelor's degree from Heilongjiang University of traditional Chinese medicine in 2003, a master's degree from Heilongjiang University of traditional Chinese medicine in 2007, and a doctor's degree from East Asia University of Korea in 2015. Her main research expertise is in cardiovascular anti-platelet therapy, laboratory diagnosis and medical engineering integration. She has written many articles for international journals and conference papers. She has published 7 papers in international journals and societies, including more than 5 SCI papers and 2 as the first author. She also presided over and participated in many projects, including the project of science and technology department of Qiqihar city in Heilongjiang province, the project of natural science foundation of Heilongjiang province, and the project of education department of Heilongjiang province.

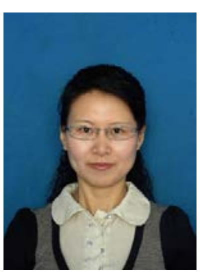

Dongmei Wei, Post doctor, PhD of medicine, Chief physician. She is the postgraduate Tutor of geriatrics in Jiamusi University. She obtained a bachelor's degree from Heilongjiang University of traditional Chinese medicine in 2004, a master's degree in 2007 and a doctor's degree in 2010. She has participated four time in the research of natural science foundation projects of the province, obtained thrice third prize of provincial science and technology progress award, twice third prize of provincial medical and health new technology application award. She published 1 monograph, and 1 SCI paper. Her research direction is the basic and applied research of traditional Chinese medicine treatment of senile diseases.

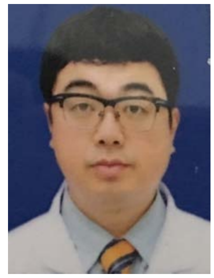

Long Zhe Guo, Post doctor, PhD of medicine, Deputy chief physician. He obtained bachelor's degree from Harbin Medical University in 2005, and obtained a master's degree in cardiovascular from Harbin medical university in 2013. He used to study in Korea to obtain a doctorate in cardiovascular medicine at the Dong-A University, South Korea in 2015. His main research expertise is in cardiovascular anti-platelet therapy, stem cell therapy and medical engineering combined research direction. He has written a number of articles for international journals and conference papers. He has published dozens of papers in international journals and societies, including more than 10 SCI papers and 7 as the first author. He has also presided over and participated in a number of projects, including the national post-doctoral project and the natural science foundation project of Heilongjiang province.

Hong Chen, Post doctor, PhD of medicine, Chief physician. He is the adjunct professor, doctoral supervisor of university of Tennessee, and master's supervisor of Heilongjiang university of traditional Chinese medicine. He obtained a bachelor's degree from Heilongjiang University of traditional Chinese medicine in 1989, a master's degree from Harbin Medical University in 2006, and a doctor's degree from Heilongjiang University of traditional Chinese medicine in 2011. He already presided over one project of provincial natural science foundation, and obtained twice third prize of provincial science and technology progress award, twice third prize of provincial medical and health new technology application award. He has published 2 monographs and 9 SCI papers, and his research direction is the basic and applied research on the treatment of cardiovascular diseases and tumors with traditional Chinese medicine with special allowance of the state council. He is also the fourth batch of famous traditional Chinese medicine in Heilongjiang province, the national second-level post expert, the leader of geriatric diseases of traditional Chinese medicine Heilongjiang provincial leading talent team, the provincial outstanding young and middle-aged expert, the provincial model worker, and "May 1" labor medalist.